

Highly Efficient and Tunable Filtering of Electrons' Spin by Supramolecular Chirality of Nanofiber-Based Materials


Chidambar Kulkarni, Amit Kumar Mondal, Tapan Kumar Das, Gal Grinbom, Francesco Tassinari, Mathijs F. J. Mabesoone, E. W. Meijer,* and Ron Naaman*

Organic semiconductors and organic–inorganic hybrids are promising materials for spintronic-based memory devices. Recently, an alternative route to organic spintronic based on chiral-induced spin selectivity (CISS) is suggested. In the CISS effect, the chirality of the molecular system itself acts as a spin filter, thus avoiding the use of magnets for spin injection. Here, spin filtering in excess of 85% in helical π -conjugated materials based on supramolecular nanofibers at room temperature is reported. The high spin-filtering efficiency can even be observed in nanofibers assembled from mixtures of chiral and achiral molecules through chiral amplification effect. Furthermore and most excitingly, it is shown that both “up” and “down” orientations of filtered spins can be obtained in a single enantiopure system via the temperature-dependent helicity (P and M) inversion of supramolecular nanofibers. The findings showcase that materials based on helical noncovalently assembled systems are modular platforms with an emerging structure–property relationship for spintronic applications.

Organic molecules have emerged as promising materials for application in spintronic devices.^[1–4] The approach of using light atoms and the small dimensions of organic molecules is very appealing in providing a possibility to have room-temperature devices with high spin selectivity. However, the development of highly efficient organic spintronic devices operating under ambient conditions is still challenging. An organic-based device with high magnetoresistance (MR) of 40% at low temperature was reported more than a decade ago.^[2] Immediately after, a room temperature device was disclosed based on tris(8-hydroxyquinolino)aluminum (Alq₃) with MR up to 10%.^[5,6]

Dr. C. Kulkarni, M. F. J. Mabesoone, Prof. E. W. Meijer
Institute for Complex Molecular Systems
Eindhoven University of Technology
P.O. Box 513, 5600 MB Eindhoven, The Netherlands
E-mail: e.w.meijer@tue.nl

Dr. A. K. Mondal, Dr. T. K. Das, Dr. G. Grinbom, Dr. F. Tassinari,
Prof. R. Naaman
Department of Chemical and Biological Physics
Weizmann Institute of Science
Rehovot 76100, Israel
E-mail: ron.naaman@weizmann.ac.il

 The ORCID identification number(s) for the author(s) of this article can be found under <https://doi.org/10.1002/adma.201904965>.

© 2020 The Authors. Published by WILEY-VCH Verlag GmbH & Co. KGaA, Weinheim. This is an open access article under the terms of the Creative Commons Attribution License, which permits use, distribution and reproduction in any medium, provided the original work is properly cited.

DOI: 10.1002/adma.201904965

Typically in organic magnetoresistance devices, the spins are injected from ferromagnetic electrodes and the current is affected by the external magnetic field.^[7] However, the exact role of the organic medium, the interfaces in the device, and how the properties of organic medium are affected by the external magnetic field are still under debate.

In recent years, another approach toward organic spintronics, which is based on the chiral-induced spin selectivity (CISS) effect was suggested.^[8,9] In this case, the chiral organic molecules themselves serve as spin filter, hence the spin filtering is not dictated by the magnetization direction of the ferromagnets alone, as seen for conventional organic spintronic devices. As a result, the difficulties one face in designing the ferromagnet–organic

interface are diminished.^[10] The spintronic devices based on CISS effect are expected to be more compact and amenable to miniaturization. The spin-polarization properties of various chiral molecules have been studied and typically the upper limit of spin selectivity was about 60% at room temperature, which corresponds to a ratio of about four to one between the two spin states.^[11–18] To realize spintronic devices based on the CISS effect, a much higher level of spin selectivity at room temperature and a way to easily switch the spin state is desired. In the past, we developed magnetic–conductive atomic force microscopy (mc-AFM) as an efficient method for studying the spin selectivity of chiral molecules. The mc-AFM measurements probe the spin selectivity of nanoscopic structures including the effect of the interface between the chiral materials and the ferromagnet used for analyzing the spin. The extent of spin polarization from mc-AFM studies is expressed as the ratio of currents with two different configurations of the magnet (up and down) at a particular voltage $[(I_{\text{up}}/I_{\text{down}})_V]$ or as percentage of spin polarization $\{[(I_{\text{up}} - I_{\text{down}})/(I_{\text{up}} + I_{\text{down}})] \times 100\}$. It is important to appreciate that the dependence of the current on the voltage applied is in the nonlinear regime and hence mc-AFM is sensitive to the spin selectivity of the conduction.

The goal of the present work is to demonstrate that using the CISS effect, indeed very high spin selectivity can be observed. We do not aim to present an actual spintronics device. Here, we present results showing unparalleled spin selection, using π -conjugated molecular materials based on coronene bisimide and tetra-amidated porphyrin cores appended with either chiral or achiral alkoxyphenyl groups (Figure 1a). Most of these

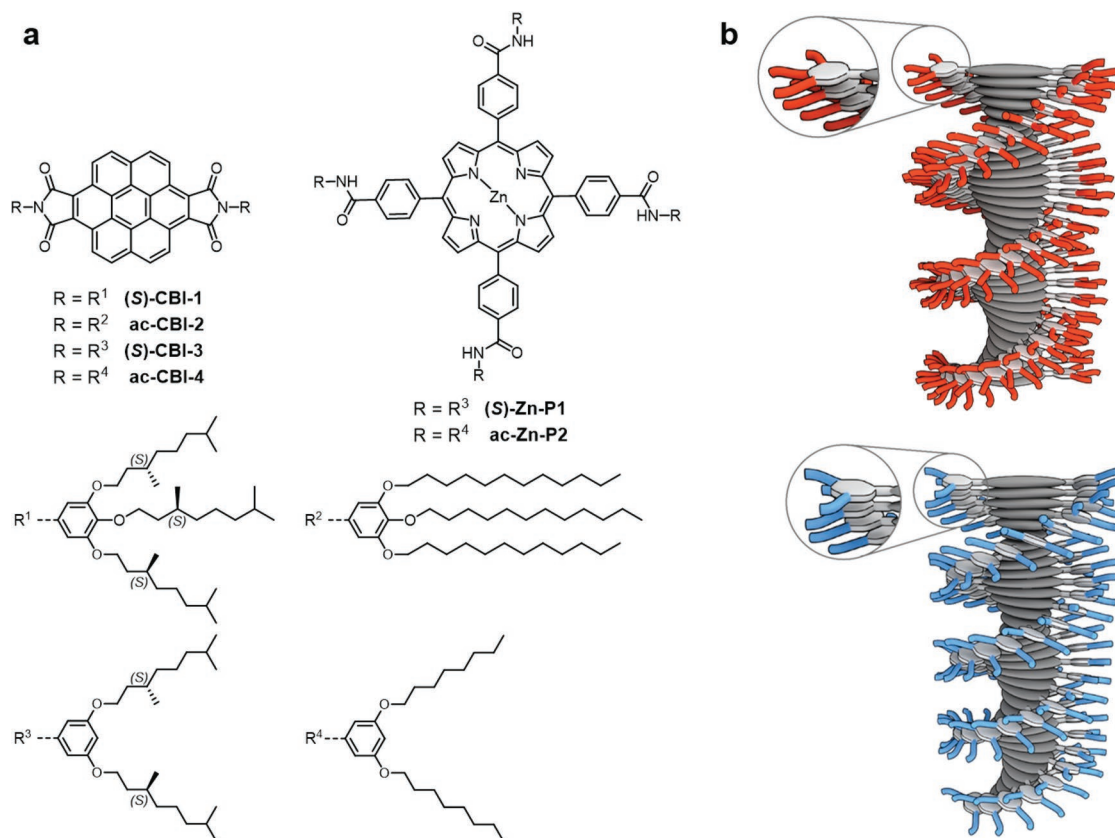


Figure 1. a) The chemical structure of the molecules involved in this study. b) Schematic representation of the self-assembled nanofibers of *P*-helicity formed by (**S**)-CBI-1 (top panel) and (**S**)-CBI-3 (bottom panel).

molecules have been studied previously and are known to form nanofibers with preferred supramolecular helicity when assembled in an apolar solvent such as methylcyclohexane (MCH).^[19–22] For systems with 3,5-dialkoxyphenyl derivatives of coronene bisimide and porphyrin ((**S**)-CBI-3 and (**S**)-Zn-P1), the spin selectivity, when measured across the cross-section of the nanofiber (10–20 nm height), reached values of up to 1:20 (85–90% spin polarization) at room temperature. In addition, we have shown CISS-based magnetoresistance device constructed from (**S**)-CBI-3 nanofibers.^[13]

A scheme representing the mc-AFM setup used in this study is shown in **Figure 2a**. The supramolecular nanofibers are formed in solution phase and transferred to a gold-coated nickel surface (Au/Ni), which is magnetized with its magnetization perpendicular to the surface with the north pole pointing either up or down. The electric potential is applied so that the AFM tip is at ground, while the potential on the Au/Ni is varied. The high resolution AFM image of the nanofibers of (**S**)-CBI-3 formed on the substrate is shown in **Figure 2b**. The height of the nanofibers as measured by AFM analysis is 17 ± 3 nm (**Figure 2c**), suggesting the bundling of individual π -stacked aggregates on the Au/Ni substrates. The studies were performed on materials based on nanofibers assembled from three chiral and three achiral molecules. The individual *I*–*V* curves are presented in **Figures S4–S9** (Supporting Information). When measuring *I* versus *V* curves, there is a force of 8–10 nN that the tip exerts on the nanofibers. For all the achiral

molecules (ac-CBI-2, ac-CBI-4, ac-Zn-P2), we did not observe any differences in the average *I*–*V* curves when the magnetic field was directed either up or down (see **Figures S5, S7, and S9** in the Supporting Information). As shown in **Figure 2d–i**, the effect of the magnetic field was remarkably pronounced for all the three chiral molecules. The (**S**)-CBI-1, with 3,4,5-trialkoxyphenyl substituents shows spin polarization of ≈ 40 –50% (**Figure 2d,g** and **Figure S4** (Supporting Information)), in the range observed for most other systems studied in the past (**Table S1**, Supporting Information).^[14,23] However, the 3,5-dialkoxyphenyl-substituted (**S**)-CBI-3 showed larger difference between the currents when switching the magnetization of the Ni layer (**Figure 2e** and **Figure S6** (Supporting Information)), resulting in spin polarization of 85–90% at +3 V (**Figure 2h**). The magnitude of spin polarization was found to be consistently >80% for films with height (or thickness) in the range of 10–40 nm (**Figure S10**, Supporting Information). The weak thickness dependence indicates that once high polarization is obtained, it persists for thicker nanofibers.

Intrigued by the large difference in spin polarization between (**S**)-CBI-1 and (**S**)-CBI-3, in spite of the very similar molecular structures, we have studied the spin polarization in nanofibers assembled from a tetra-amidated porphyrin with 3,5-dialkoxyphenyl wedges ((**S**)-Zn-P1) as well. (**S**)-Zn-P1 also showed a high ratio of 20:1 for the currents with magnet up and down at +3 V (**Figure 2f** and **Figure S8** (Supporting Information)), whereas the 3,4,5-trialkoxyphenyl-substituted Zn porphyrin was

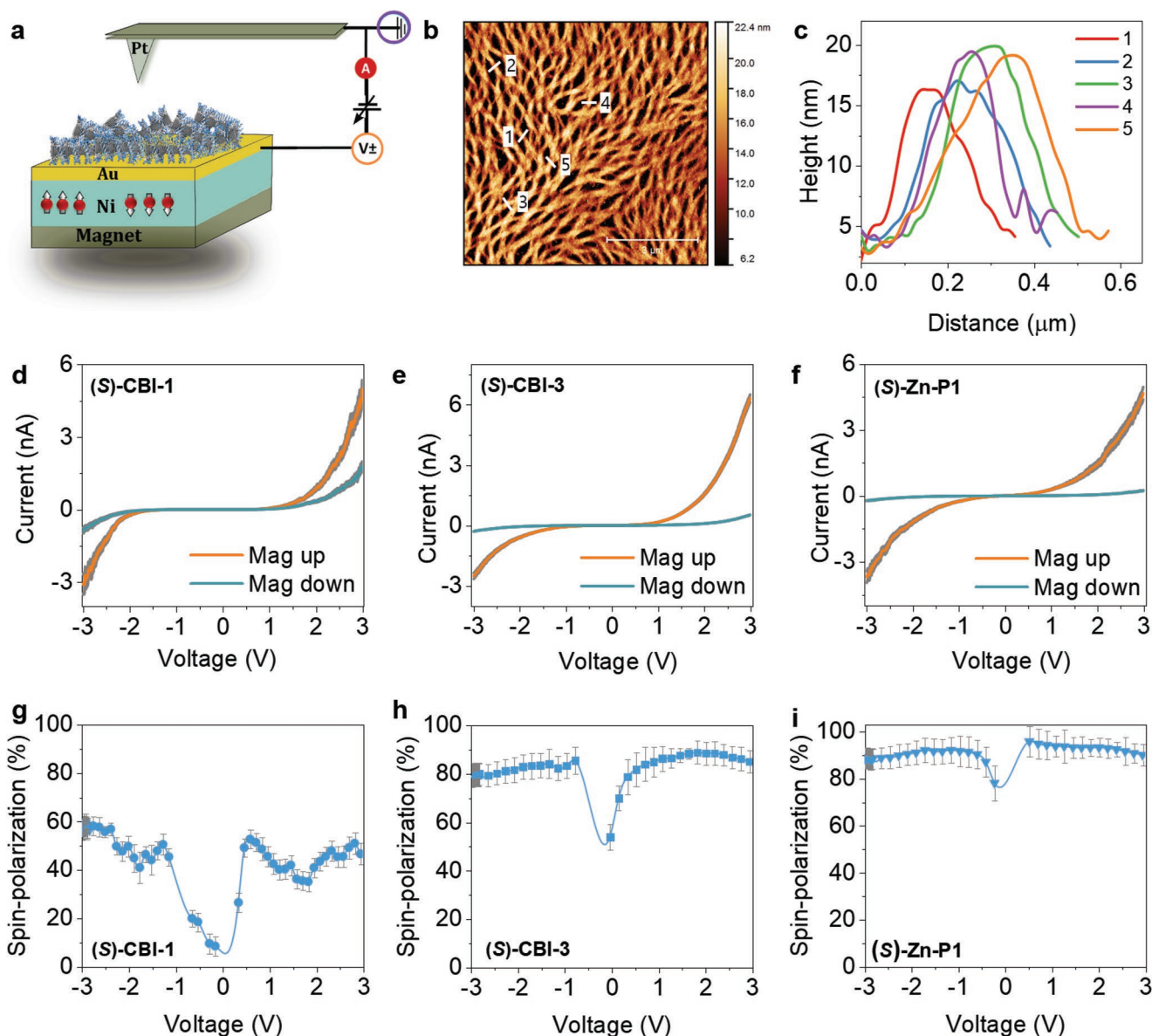


Figure 2. Spin-dependent conduction through supramolecular nanofibers of various systems. a) Schematic of the magnetic–conductive atomic force microscopy (mc-AFM) setup used to measure spin polarizations. b) High-resolution AFM image of the supramolecular structures obtained from (S)-CBI-3 drop cast on Au/Ni (10/120 nm) substrate. The scale bar in (b) is 3 μm . c) The height profiles measured along different lines shown in (b). d–f) The averaged I – V plots of (S)-CBI-1, (S)-CBI-3, and (S)-Zn-P1, respectively, with the Ni film magnetized with the north pole pointing up (orange) or down (cyan). g–i) The corresponding percentage of spin polarization $\{[(I_{\text{up}} - I_{\text{down}})/(I_{\text{up}} + I_{\text{down}})] \times 100\}$ for (S)-CBI-1, (S)-CBI-3, and (S)-Zn-P1, respectively. Here I_{up} and I_{down} are the currents with magnetic north pole up and down, respectively. Roughly 80–100 I – V curves were obtained for each molecule (see the Supporting information) and the average was obtained by summing all the curves and dividing by their number. The standard error of the average I – V curves is shown in gray color.

previously shown to exhibit spin polarization of 40%.^[24] Hence, for both coronene bisimides and tetra-amidated porphyrin systems, molecules with 3,4,5-trialkoxyphenyl substituents lead to low spin selectivity of ≈ 40 –50% (3:1), whereas systems bearing the 3,5-dialkoxyphenyl wedge consistently showed a remarkably high spin selectivity ($>85\%$ – 20:1).

The difference in spin selectivity between (S)-CBI-1 and (S)-CBI-3 (as well as for the tetra-amidated porphyrins) is unexpected and not easy to rationalize. However, it cannot be

a coincidence. Scanning tunneling microscopy (STM) studies on molecular hexapods containing six oligo(*p*-phenylene vinylene) (OPV) on a central benzene showed that one or two of the OPV units are desorbed from surface or invisible in STM images, mostly due to steric congestion.^[25] Based on these STM studies, a possible rationale for the difference in spin selectivity between (S)-CBI-1 and (S)-CBI-3 can be attributed to the difference in the packing of molecules in the nanofibers. For molecules having an alkoxyphenyl-wedge with three alkyl chains, it

is anticipated that one of the alkoxy chains is oriented out of the phenyl ring plane to minimize the steric interactions of the three alkoxy chains in close proximity. Consequently, the steric hindrance between the two consecutive molecules of **(S)**-CBI-1 in the nanofiber is proposed to lead to a more loose packing of monomers, whereas for **(S)**-CBI-3, which is substituted with 3,5-dialkoxyphenyl wedges, the packing of monomers in a nanofiber is expected to be more compact. Similar packing arguments can account for the difference in spin selectivity observed for 3,5-dialkoxyphenyl- and 3,4,5-trialkoxyphenyl-substituted Zn porphyrins.

Having shown high spin selectivity of electron transport in materials based on supramolecular nanofibers of **(S)**-CBI-3, we further developed strategies where both the efficiency of spin polarization and the polarity/orientation of the spins filtered through the nanofiber can be modulated. For the former, we have made use of the well-known “Sergeant-and-Soldier” principle of chiral amplification.^[26,27] Here, mixing chiral and achiral building blocks leads to the amplification in the net helicity of the stacks; in other words, the chiral molecule determines the supramolecular chirality of the helix and the achiral molecules follow the helicity of the chiral one. Sergeant-and-soldier experiments were performed with **(S)**-CBI-3 and **ac**-CBI-4 using circular dichroism (CD) spectroscopy (Figure S11, Supporting Information). As shown in Figure 3a, the molar circular dichroism ($\Delta\epsilon$) shows a nonlinear dependence on the fraction of **(S)**-CBI-3 in the solution, confirming the chiral amplification in the system. This chiral amplification is also expressed in the spin polarization of electron transport measured via mc-AFM studies on nanofibers drop cast on Au/Ni (10/120 nm) substrates from mixtures of **(S)**-CBI-3 and **ac**-CBI-4 at various compositions (Figure S12 and Table S2, Supporting Information). Up to 30% of **(S)**-CBI-3, we find a nonlinear increase of spin polarization, strongly resembling the trend observed in the CD studies. At and beyond 50% of **(S)**-CBI-3, the magnitude of spin polarization is comparable to that observed for nanofibers assembled from enantiomerically pure **(S)**-CBI-3 (Figure 3b). Remarkably, there is a direct correlation between the changes observed in the CD signal and the spin polarization measured from mc-AFM as a function of fraction of **(S)**-CBI-3. These results indicate that chiral amplification principles can be used to control the magnitude of spin polarization of helical nanofibers. Moreover, the results directly prove that the CISS effect is the result of the supramolecular chirality and not just due to the number of stereocenters present in the film.

In addition to achieving and controlling high spin selectivity, it is paramount to modulate the polarity of the spins transferred through the system. Typically, this is achieved by using two enantiopure forms of the molecular system. By contrast, here we explored the possibility of attaining both “up” and “down” polarity/orientation of spins transported in a single enantiopure system via conformational changes to the supramolecular nanofibers. An interesting indication of the correlation between the molecular structure, sign of CD signal (supramolecular chirality), and the spin polarization is provided when the **(S)**-CBI-3 molecules are assembled in methylcyclohexane at $-10\text{ }^{\circ}\text{C}$ instead of $20\text{ }^{\circ}\text{C}$. While at $20\text{ }^{\circ}\text{C}$ the Cotton effect at longer wavelength ($\approx 500\text{ nm}$) was positive

(Figure 3c), indicative of (*P*)-helical stacks, at $-10\text{ }^{\circ}\text{C}$, the CD spectrum changes sign over the entire absorption range, indicating the formation of (*M*)-helical stacks (Figure 3c,d). Due to the 3,5-position of the alkoxy chains on the phenyl groups, the **(S)**-CBI-3 molecule possesses a pocket accessible to solvents. It has been previously shown that the formation of inclusion type of complexes between the solvent and the molecular pocket of an assembly leads to dynamic stereomutation at low temperature, or in other words a conformational change from (*P*)- to (*M*)-helicity of nanofibers.^[20]

The temperature-dependent conformational changes observed for **(S)**-CBI-3 is used to investigate the spin-dependent electron conduction through **(S)**-CBI-3 nanofibers prepared at different temperatures. For the nanofibers assembled at room temperature, the highest current was obtained when the magnet is pointing up (preferred spin is aligned antiparallel to the electron's velocity, Figure 3e). However, for **(S)**-CBI-3 nanofibers which were assembled at $-10\text{ }^{\circ}\text{C}$, the highest current was obtained when the magnet is pointing down (preferred spin is aligned parallel to the electron's velocity, Figure 3f and Figure S12 (Supporting Information)). It is worth noting that the efficiency of spin polarization remains $>80\%$ for **(S)**-CBI-3 nanofibers assembled at both $+20$ and $-10\text{ }^{\circ}\text{C}$ (Figure S13, Supporting Information). This again clearly indicates that the spin orientation of electrons transferred through **(S)**-CBI-3 nanofibers depends on the supramolecular helicity of the stacks, which can in turn be modulated by a temperature-induced conformational change.

Finally, we constructed a prototype device for measuring the MR following the ref. [13] (see details in the Supporting Information). Figure 4 shows a scheme of the device structure and the results obtained using the materials from nanofibers of **(S)**-CBI-3. A clear signature of magnetoresistance is observed, when the curve is asymmetric relative to the magnetic field direction (Figure 4b). This is a result of having only a single magnetic layer in the device and the spin selectivity of the chiral structures. The MR is temperature independent as always observed in CISS-based MR devices.^[13,14] Furthermore, MR devices constructed from achiral **ac**-CBI-4 as the active layer showed a symmetric profile (Figure S14, Supporting Information), reaffirming that chirality of the molecular systems leads to asymmetric MR as observed for **(S)**-CBI-3. The relatively low magnetoresistance is explained by the large area of the electrodes which results in collecting electrons that are passed through pin holes in the chiral layer or were scattered as well. These problems do not exist in the mc-AFM configuration, where the conduction at the nanoscale is probed and hence there much higher spin selectivity was observed. Optimizing the device architecture is required to get similar high effects in the devices.

In the present work, we have shown that supramolecular materials in the form of nanofibers behave as extremely efficient spin filters, when the current is conducted perpendicular to the long axis of the nanofiber, i.e., across the diameter. The thickness of the nanofiber measured indicates that tens of molecules or more than one nanofibers are involved in the conduction process. The extremely high spin polarization obtained may result from sequential transfer of the electrons through several molecules, with spin selectivity taking place in each

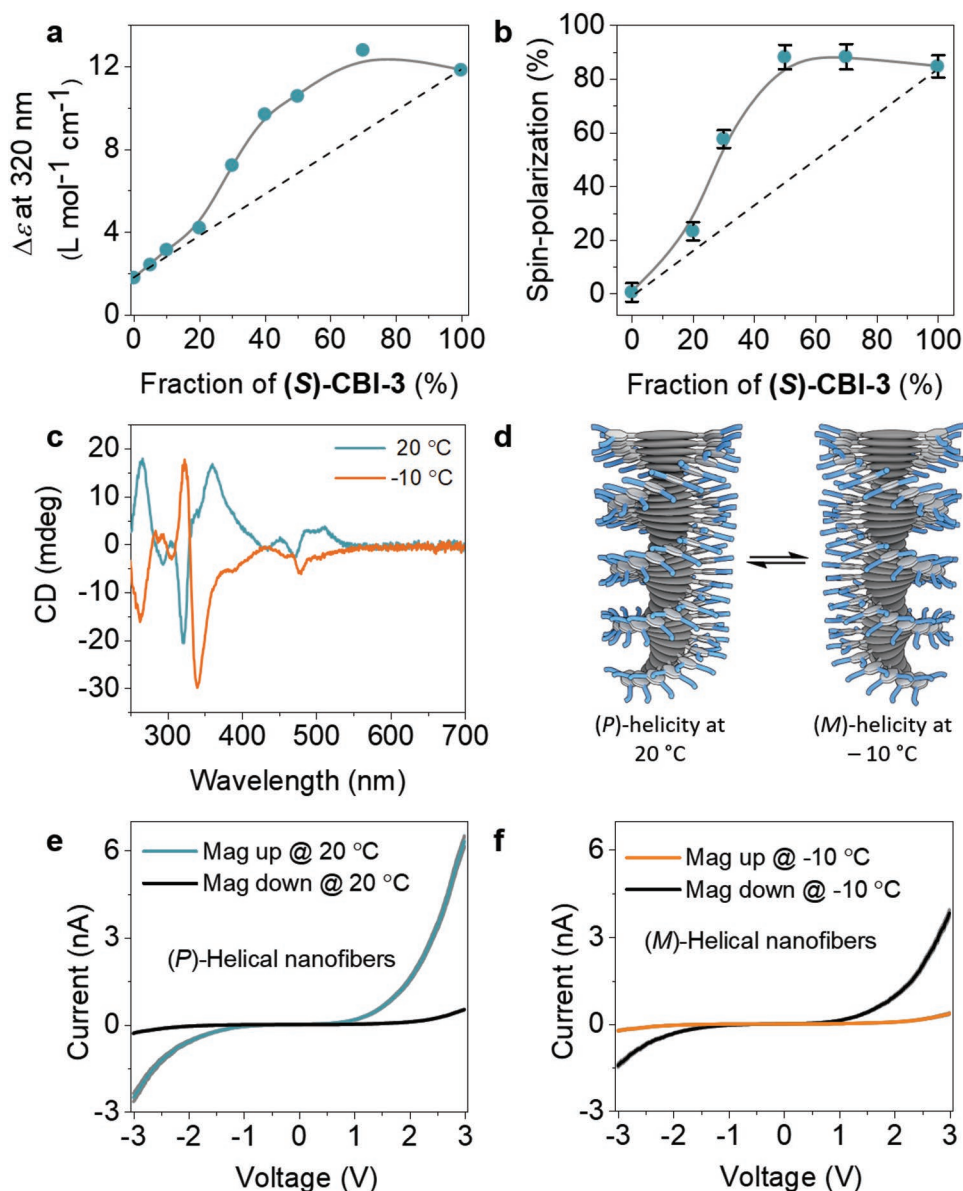


Figure 3. Controlling the spin selectivity through chiral amplification and conformational change. a) Evolution of the molar circular dichroism ($\Delta\epsilon$) as a function of fraction of sergeant ((S)-CBI-3) in a sergeant and soldier experiment involving (S)-CBI-3 and ac-CBI-4 ($c = 50 \times 10^{-6}$ M in MCH at 20 °C), as measured by circular dichroism spectroscopy. The nonlinear dependence of $\Delta\epsilon$ on the fraction of sergeant suggests chiral amplification in the solution-state assembly processes. b) Spin polarization at +3 V measured using mc-AFM-based I - V curves at different fractions of (S)-CBI-3 in nanofibers made from a mixture of (S)-CBI-3 and ac-CBI-4. The same solutions used for CD studies were used for the formation of the nanofibers by drop casting on Au/Ni (10/120 nm) substrates. The solid-gray lines in (a) and (b) are a guide to the eye. The dashed black line indicates the expected trend in data in the absence of chiral amplification. c) Temperature-dependent CD spectra of (S)-CBI-3 ($c = 50 \times 10^{-6}$ M in MCH). d) Schematic illustrating the change in helicity of supramolecular nanofibers upon changing the temperature from +20 to -10 °C. e, f) The averaged I - V curves of (S)-CBI-3 ($c = 20 \times 10^{-6}$ M in MCH) when drop cast on a Au/Ni substrate at +20 and -10 °C, respectively. The standard error of the average I - V curves in (e) and (f) is shown in gray color. The mc-AFM measurements were performed at room temperature.

molecule and the spin alignment does not undergo dephasing during transport through the molecules. Hence, a multistage spin filtering takes place.

These studies clearly demonstrate that the spin selectivity originates from helical supramolecular nanofibers rather than individual chiral molecules. Although spin selectivity was previously observed in supramolecular nanofibers,^[24]

here we show for the first time that there is a strong correlation between the molecular structure of the materials, their chiral supramolecular assembly, and consequently the spin-polarization efficiency. The electronically passive, solubilizing part of the molecules, i.e., the 3,5-dialkoxyphenyl wedge, which imparts high spin selectivity to (S)-CBI-3 and (S)-Zn-P1, might serve as a conduit to achieve high spin selectivity

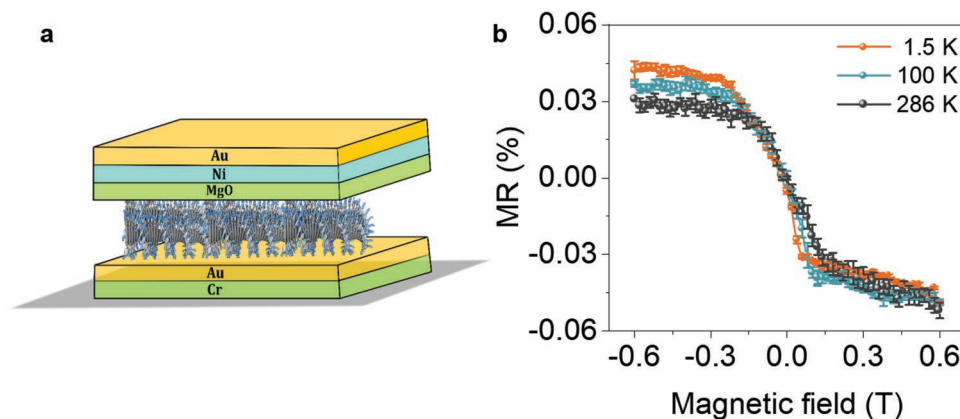


Figure 4. Solid-state magnetoresistance device studies. a) Schematic representation of the magnetoresistance device. b) Magnetoresistance curves for (S)-CBI-3 nanofibers as a function of magnetic field between -0.6 and 0.6 T at different temperatures. The measurements were performed at a constant current of 2.5 mA. The MR curves were obtained by measuring the voltage while sweeping the magnetic field.

in other systems as well. The results shown here provide an important indication that the CISS effect in chiral organic materials can lead to efficient spintronics elements at room temperature. Because of the high efficiency, about 20 nm thick layer of supramolecular helical nanofibers can provide spin filtering not easily obtained with inorganic devices even at low temperatures.

Supporting Information

Supporting Information is available from the Wiley Online Library or from the author.

Acknowledgements

C.K., M.F.J.M., and E.W.M. thank financial support from the NWO (TOP-PUNT Grant No. 10018944) and the Dutch Ministry of Education, Culture, and Science (Gravitation Program 024.001.035). The authors thank Prof. Anja R. A. Palmans and Prof. Subi J. George for fruitful discussions. C.K. acknowledges the Marie Skłodowska-Curie postdoctoral fellowship (Grant No. 704830) for financial support. R.N. acknowledges the partial support by the VW Foundation, the Israel Science Foundation, and the Israel Ministry of Science. The authors thank Dr. Sidney R. Cohen and Dr. Suryakant Mishra for fruitful discussions.

Conflict of Interest

The authors declare no conflict of interest.

Author Contributions

C.K. and A.K.M. contributed equally to this work. C.K., E.W.M., and R.N. conceived the project. C.K. carried out the synthesis and solution-phase assembly studies of CBI molecules. A.K.M. carried out the mc-AFM experiments. C.K. and A.K.M. together optimized sample preparation for helicity-reversal mc-AFM experiments. T.K.D., G.G., and F.T. performed magnetoresistance measurements. M.F.J.M. contributed materials (ac-Zn-P2) and schematics for the figures. C.K., E.W.M., and R.N. wrote the paper with input from all the coauthors. E.W.M. and R.N. supervised the overall project.

Keywords

CISS effect, nanofibers, spin filtering, supramolecular chirality

Received: August 1, 2019
Revised: November 13, 2019
Published online: January 10, 2020

- [1] C. Hermann, G. C. Solomon, M. A. Ratner, *J. Am. Chem. Soc.* **2010**, *132*, 3682.
- [2] Z. H. Xiong, D. Wu, Z. V. Vardeny, J. Shi, *Nature* **2004**, *427*, 821.
- [3] K. V. Raman, A. M. Kamerbeek, A. Mukherjee, N. Atodiresei, T. K. Sen, P. Lazić, V. Caciuc, R. Michel, D. Stalke, S. K. Mandal, S. Blügel, M. Münzenberg, J. S. Moodera, *Nature* **2013**, *493*, 509.
- [4] L. Guo, X. Gu, X. Zhu, X. Sun, *Adv. Mater.* **2019**, *31*, 1805355.
- [5] V. Dediu, L. E. Hueso, I. Bergenti, A. Riminucci, F. Borgatti, P. Graziosi, C. Newby, F. Casoli, M. P. De Jong, C. Taliani, Y. Zhan, *Phys. Rev. B* **2008**, *78*, 115203.
- [6] V. A. Dediu, L. E. Hueso, I. Bergenti, C. Taliani, *Nat. Mater.* **2009**, *8*, 707.
- [7] P. A. Bobbert, T. D. Nguyen, F. W. A. Van Oost, B. Koopmans, M. Wohlgenannt, *Phys. Rev. Lett.* **2007**, *99*, 216801.
- [8] K. Michaeli, N. Kantor-Uriel, R. Naaman, D. H. Waldeck, *Chem. Soc. Rev.* **2016**, *45*, 6478.
- [9] R. Naaman, Y. Paltiel, D. H. Waldeck, *Nat. Rev. Chem.* **2019**, *3*, 250.
- [10] C. Barraud, P. Seneor, R. Mattana, S. Fusil, K. Bouzehouane, C. Deranlot, P. Graziosi, L. Hueso, I. Bergenti, V. Dediu, F. Petroff, A. Fert, *Nat. Phys.* **2010**, *6*, 615.
- [11] B. Göhler, V. Hamelbeck, T. Z. Markus, M. Kettner, G. F. Hanne, Z. Vager, R. Naaman, H. Zacharias, *Science* **2011**, *331*, 894.
- [12] M. Kettner, B. Göhler, H. Zacharias, D. Mishra, V. Kiran, R. Naaman, C. Fontanesi, D. H. Waldeck, S. Sek, J. Pawowski, J. Juhaniwicz, *J. Phys. Chem. C* **2015**, *119*, 14542.
- [13] S. P. Mathew, P. C. Mondal, H. Moshe, Y. Mastai, R. Naaman, *Appl. Phys. Lett.* **2014**, *105*, 242408.
- [14] V. Kiran, S. P. Mathew, S. R. Cohen, I. Hernández Delgado, J. Lacour, R. Naaman, *Adv. Mater.* **2016**, *28*, 1957.
- [15] J. M. Abendroth, K. M. Cheung, D. M. Stemer, M. S. El Hadri, C. Zhao, E. E. Fullerton, P. S. Weiss, *J. Am. Chem. Soc.* **2019**, *141*, 3863.
- [16] K. M. Alam, S. Pramanik, *Adv. Funct. Mater.* **2015**, *25*, 3210.

- [17] M. Á. Niño, I. A. Kowalik, F. J. Luque, D. Arvanitis, R. Miranda, J. J. de Miguel, *Adv. Mater.* **2014**, *26*, 7474.
- [18] M. Suda, Y. Thathong, V. Promarak, H. Kojima, M. Nakamura, T. Shiraogawa, M. Ehara, H. M. Yamamoto, *Nat. Commun.* **2019**, *10*, 2455.
- [19] C. Kulkarni, R. Munirathinam, S. J. George, *Chem. - Eur. J.* **2013**, *19*, 11270.
- [20] C. Kulkarni, P. A. Korevaar, K. K. Bejagam, A. R. A. Palmans, E. W. Meijer, S. J. George, *J. Am. Chem. Soc.* **2017**, *139*, 13867.
- [21] R. van der Weegen, A. J. P. Teunissen, E. W. Meijer, *Chem. - Eur. J.* **2017**, *23*, 3773.
- [22] F. Helmich, C. C. Lee, M. M. L. Nieuwenhuizen, J. C. Gielen, P. C. M. Christianen, A. Larsen, G. Fytas, P. E. L. G. Leclère, A. P. H. J. Schenning, E. W. Meijer, *Angew. Chem., Int. Ed.* **2010**, *49*, 3939.
- [23] T. J. Zwing, S. Hürlimann, M. G. Hill, J. K. Barton, *J. Am. Chem. Soc.* **2016**, *138*, 15551.
- [24] W. Mtangi, F. Tassinari, K. Vankayala, A. Vargas Jentzsch, B. Adelizzi, A. R. A. Palmans, C. Fontanesi, E. W. Meijer, R. Naaman, *J. Am. Chem. Soc.* **2017**, *139*, 2794.
- [25] H. Xu, A. Minoia, Ž. Tomović, R. Lazzaroni, E. W. Meijer, A. P. H. J. Schenning, S. De Feyter, *ACS Nano* **2009**, *3*, 1016.
- [26] M. M. Green, M. P. Reidy, R. J. Johnson, G. Darling, D. J. O'Leary, G. Willson, *J. Am. Chem. Soc.* **1989**, *111*, 6452.
- [27] A. R. A. Palmans, E. W. Meijer, *Angew. Chem., Int. Ed.* **2007**, *46*, 8948.